Evaluation and Analysis of the Wi-Fi HaLow Energy Consumption

Sébastien Maudet, Guillaume Andrieux, Romain Chevillon, and Jean-François Diouris

***Abstract*—One of the key issues with the Internet of Things (IoT) is energy consumption. This type of network is mainly composed of connected objects supplied by an unreliable power source. Wi-Fi HaLow is one of the telecommunication technologies that proposes to connect IoT objects by providing energy optimization mechanisms. It allows the integration of a full IP stack and the implementation of recent security mechanisms. In this article, we introduce power consumption measurements performed on the first device available on the market. In our study, we integrate the current consumed by the power amplifier in transmission phase, and we qualify the power-saving mechanisms. We then propose an analytical model to determine the energy consumed by a sensor node depending on the carried payload. Finally, we validate the use of this technology in IoT application in terms of energy consumption.**

***Index Terms*—Energy consumption, IEEE 802.11ah, Internet of Things (IoT), Wi-Fi HaLow, wireless sensor network (WSN).**

I. Introduction

THE Internet of Things (IoT) is an innovative concept of connecting objects to a network. This vision has imposed new challenges for designers. First, IoT networks must support a large number of heterogeneous devices, while ensuring fair access. Second, these devices are often powered by unreliable energy sources, requiring new mechanisms to optimize energy consumption. The 802.11ah, also called Wi-Fi HaLow, is one of the technologies designed for IoT, with several mechanisms that are adopted to limit collisions, increase the number of devices and minimize energy consumption. Much work has been done by the scientific community in modeling and simulation, but few practical evaluations have been proposed due to the lack of equipment. In this article, we perform a comprehensive power consumption evaluation using the first commercially available chip to validate the use of 802.11ah in IoT applications. All the acronyms that are used in this article are listed in Table I.

TABLE I
List of Acronyms

Acronyms	Description
AID	Association IDentifier
A-MPDU	Aggregate MAC Protocol Data Unit
AP	Access Point
ARP	Address Resolution Protocol
BW	BandWidth
CSMA/CA	Carrier Sense Multiple Access / Collision Avoidance
DCF	Distributed Coordination Function
DIFS	Distributed Inter-Frame Space
DL MU-MIMO	DownLink Multi-User MIMO
EDCA	Enhanced Distributed Coordination Access
EVK	EValuation Kit
FEM	Front End Module
FOTA	Firmware Over The Air
HT	High Thoughput
IP	Internet Protocol
LP-WAN	Low Power Wide Area Network
MAC	Media Access Control
MCS	Modulation and Coding Scheme
MIMO	Multiple Input Multiple Output
MPDU	MAC Protocol Data Unit
NAV	Network Allocation Vector
NDP	Null Data Packet
OFDM	Orthogonal Frequency Division Multiplexing
PHY	PHYsical
PRAW	Periodic RAW
PS	Power Save
QoS	Quality of Service
RAW	Restricted Access Windows
SIG	SIGnal
SoC	System on Chip
STA	STAtion
SIFS	Short Inter-Frame Space
SSL/TLS	Secure Socket Layer / Transport Layer Security
TCP	Transport Control Protocol
TDMA	Time Division Multiple Access
TGah	Task Group of 802.11ah
TIM	Target Indication Map
TWT	Target Wake Time
TWT-SP	Target Wake Time - Service Periods
TxOP	Transmission OPortunity
UDP	User Datagram Packet
WPA	Wi-Fi Protected Access
WPAN	Wireless Personal Area Network
XiP	eXecution in Place

A. Related Works

Many works in the literature give an overview of the main 802.11ah characteristics [1], [2], [3]. Khorov et al. [4] investigated and adapt several mechanisms through an analytical study. In [5], they complete their survey with numerical results that justify the use of this technology in IoT. A survey is also proposed by [6], [7], and [8] with a synthesis of the challenges and promising research directions. Wessel and Vries [9] evaluated theoretical throughput and transmission range for indoor and outdoor environments. In [10] and [11], they propose a theoretical model to limit power consumption

Manuscript received 1 February 2024; revised 16 March 2024; accepted 4 May 2024. Date of publication 16 May 2024; date of current version 23 August 2024. This work was supported in part by the La Roche-sur-Yon Agglomération, Région Pays-de-la-Loire, and the European Union through the European Regional Development Fund (ERDF) as part of the WISE'Labs Platforms, and in part by the French National Research Agency as part of France 2030 and the NF-FITNESS Project under Grant ANR-22-PEFT-0007. *(Corresponding author: Sébastien Maudet.)*

The authors are with the Nantes Université, CNRS, IETR, UMR 6164, 85000 La Roche-sur-Yon, France (e-mail: sebastien.maudet@univ-nantes.fr).

Digital Object Identifier 10.1109/JIOT.2024.3401862

and to determine the maximum number of stations based on traffic conditions.

Other works present modeling, or propose new mechanisms to optimize metrics and energy consumption [12], [13], [14], [15]. In [16], a media access control (MAC) scheme with a power saving mechanism is developed. Wang et al. [17], Yanru et al. [18], and Wang et al. [19] provided an energy-sensitive window control algorithm to adjust the restricted access windows (RAWs) size and find the optimal number of devices. In [20], a stochastic energy consumption model is used to calculate the expected lifetime of a sensor node. Beltramelli et al. [21] combined a mathematical power consumption model with a contention-reservation MAC mechanism. In [22], they intend to reduce access times and energy consumption by predicting the service interval and scheduling the subsequent frames.

Some other works deal with the promising MAC mechanisms. Bankov et al. [23] and Kao et al. [24] studied the average transmission time, the packet loss rate and the energy consumed in target wake time (TWT). The target indication map (TIM) mechanism is investigated in [25] and [26]. The first introduces a decentralized clustering algorithm and the second studies the impact on a saturated traffic network. Bel et al. [27] forward a novel channel access protocol in which the RAWs can be divided. The RAW is also studied in [28], with an optimal configuration in a scenario with a large number of energy harvesting stations. Zhang and Yeung [29] improved the distributed coordination function (DCF) with a timing mechanism in case of pending alarm reports and Gopinath and Nithya [30] investigate a new backoff algorithm. In [31], a TIM and RAW cooperation is suggested for a large number of low-power devices network. However, none of these works validate their proposals with real-world energy measurements due to the lack of equipment on the market. In most cases, they assume that the wake-up and transmission phases of the various devices are instantaneous.

To the best of our knowledge, only one paper proposes power consumption measurements on a real system. Lee et al. [32] validated the Wi-Fi HaLow technology as a long-range IoT solution with high throughput and low-power consumption. However, they do not consider the evolution of the power consumed by the different elements of a STA during a complete transmission phase.

B. Contributions and Organization

This article introduces energy consumption experiments performed on the first available 802.11ah hardware. This work is unique in several ways: 1) in-situ measurements of the power consumed by the various elements of an IoT sensor are made; 2) these measurements are analyzed and compared with the theoretical values; and 3) the results are used to determine the lifetime of an IoT sensor and the energy consumed per useful bit.

This article is organized as follows: the main features of the Wi-Fi HaLow are described in Section II. Section III presents in-situ measurements that permit the evaluation of the node energy consumption. Section IV introduces a simple model and an open discussion about the energy. Finally, we draw a conclusion in Section V.

TABLE II
OFDM MODULATION CHARACTERISTICS IN 802.11AH AND 802.11AC

	Mod.	BandWidth (BW)	T_{GI}	T_{SYMB}
802.11ah	OFDM	1/2/4/8/16 MHz	4/8 µs	32 µs
802.11ac	OFDM	20/40/80/160 MHz	0.4/0.8 µs	3.2 µs

II. Wi-Fi HaLow Technology

A. Wi-Fi HaLow Overview

A Wi-Fi network is composed of STAtions (STA) connected to an access point (AP) in a star topology. It provides the functions of the media access layers and fills the gap between low-power wide area network (LP-WAN) and wireless personal area network (WPAN). Data rates and latency allow it to be used in various IoT applications, from e-health to Industry 4.0, smart grid and smart agriculture [2], [8], [33]. Unlike other IoT protocols, dot11ah is a transport control protocol/Internet protocol (TCP/IP) native technology which enables the implementation of advanced security mechanisms, such as secure socket layer/transport layer security (SSL/TLS) and Wi-Fi protected access (WPA3). The standard defines three typical use cases [7], [8], [34]: 1) sensors and meters; 2) backhaul for other sensor networks; and 3) extended range Wi-Fi applications. In this article, we focus on the first use case for its operating and lifetime constraints.

B. Wi-Fi HaLow PHY Layer Overview

At the PHYsical (PHY) layer, transmissions are performed in sub-GHz frequency bands using orthogonal frequency division multiplexing (OFDM) [8]. The physical characteristics are divided by 10 compared to the 802.11ac, as shown in Table II. With these theoretical features, the data rate can vary from 150 Kb/s to 78 Mb/s and the distance can reach 1 km [33]. multiple-input multiple-output (MIMO), beamforming and downlink multiple user MIMO (DL MU-MIMO) techniques can also be implemented to promote spatial diversity and improve the data rate [25], [32].

C. Wi-Fi HaLow MAC Layer Overview

At the MAC layer, the goal is to increase the number of STAs in the network and decrease the amount of energy consumed. To achieve this, four mechanisms have been created or improved from the legacy: 1) the hierarchical association ID (AID); 2) the TIM; 3) the RAW; and 4) the TWT. These mechanisms will be detailed in the following sections. The 802.11ah media access methods are based on the legacy DCF and enhanced distributed coordination access (EDCA) [7], [35]. EDCA is an extension of DCF that prioritizes traffic to ensure Quality of Service (QoS). In the Wi-Fi HaLow, four QoS categories have been defined for sensors and four others for various types of STAs [36]. These media access mechanisms are specifically those used in the TIM, RAW and TWT slots.

D. Scalability and Power Saving MAC Mechanisms

1) Types of STA: Three types of STAs can coexist in a 802.11ah network [1], [5], [7].

1) TIM STAs must receive TIM beacon frames and can transmit data in a RAW slot. These two mechanisms aim to minimize collisions and optimize power consumption. TIM STAs have a high-traffic throughput.
2) Non TIM STAs do not need to wake up to receive TIM beacon frames. They can negotiate their transmission times directly with the AP. Non TIM STAs have a strong need to conserve energy.
3) Unscheduled STAs can transmit whenever they want and request immediate access to the AP. Unscheduled STAs require sporadic access to the network.

2) Hierarchical AID: In a traditional Wi-Fi network, each STA is identified by a 11-bit AID, which allows $2^{11} = 2048$ various connected STAs. In the 802.11ah, this AID is encoded with 13 bits, increasing the number of identifiable STAs to $2^{13} = 8192$ [6], [31]. The design of this AID allows STAs to be grouped according to their traffic, latency, geographic area or energy [6], [7].

3) Short Header and Null Data Packet: Two solutions are proposed to reduce frame duration and thus minimize energy consumption. The first defines a new PV1 MAC header containing 10 to 26 bytes, instead of the 40 bytes of the legacy PV0. This is done by addressing the source and the destination with either the 2-byte AID or the 6-byte MAC address, and removing the QoS and high thoughput (HT) control fields [1], [7]. The second solution is called null data packet (NDP). These packets contain only a PHY layer and no MAC header. The useful information of the MAC header is placed in the SIGnal (SIG) field of the PHY header, thus reducing some NDP control frames to 6 symbols (i.e., 240 μs) in the case of 2-MHz BW and 14 symbols (i.e., 560 μs) in the case of 1-MHz BW [1], [6], [7].

4) Traffic Indication Map Segmentation: In legacy, TIM elements are embedded in the beacon to inform power save (PS) STAs that there are buffered frames in the AP. The TIM information consists of a virtual bitmap field where the STAs are indexed by bit positioning. To receive the buffered traffic, the STAs must wake up and receive the TIM beacon frames. If they are indexed in the TIM elements, they send a PS-poll to the AP, which responds with the buffered data frame. In 802.11ah, the large number of STAs and the need to conserve power do not allow devices to wake up to receive each TIM beacon. To solve this problem, the 802.11ah introduces TIM segmentation where TIM elements are divided into multiple fragments, each transmitted in a single TIM beacon frame. As shown on Fig. 1, the DTIM beacon indicates the data pending for the groups in its bitmap, and the TIM beacon frames specify the STAs of the group involved. STA 522 wake up for the TIM beacon because its group is indicated in the DTIM. STA 522 send a PS-poll to receive the buffered traffic because it is specified in the TIM beacon. Other STAs may remain in sleep state until the next DTIM announcement [1], [6], [7], [10], [11].

5) Restricted Access Window: RAW is related to the TIM mechanism. It allows an AP to allocate a RAW time slot to a group of TIM STAs, in which they are allowed to access the media. RAW is a combination of EDCA and time division multiple access (TDMA). In this process, the AP informs the STAs of its RAW slot by adding RAW Parameter Set elements in the TIM beacon frame. The STA can then access the media in its reserved RAW slot using the DCF and EDCA mechanisms. RAW can minimize collisions, save energy and promote fairness when a large number of sensors try to access the media at the same time [1], [6], [7], [10], [11].

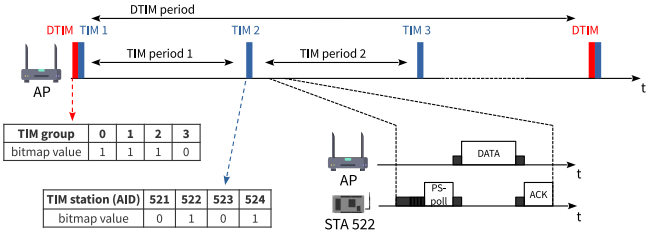

Fig. 1. 802.11ah TIM segmentation mechanism.

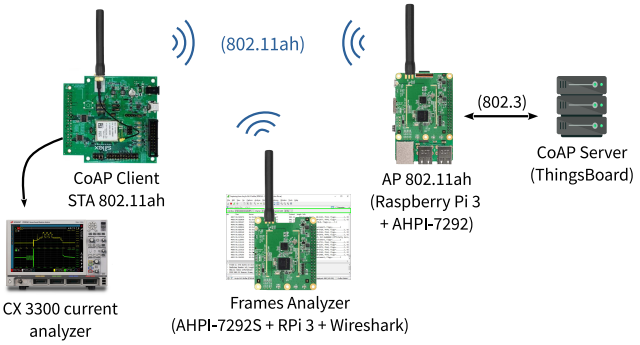

Fig. 2. 802.11ah current measurements testbed.

6) Target Wake Time: TWT is another power saving mechanism that allows STAs with sporadic data transmissions to negotiate their wake-up service periods with the AP. In this process, STAs need to be awake for each TWT-service period (TWT-SP) and not to receive TIM beacons. The STA and the AP can negotiate the time of the first TWT-SP and a regular average TWT wake-up interval or the next TWT-SP in each TWT-SP. A TWT agreement may authorize uplink and/or downlink transmissions, and the STAs must use the DCF and EDCA mechanisms to access the media. The AP protects a TWT-SP by using periodic RAW (PRAW) and the legacy network allocation vector (NAV) mechanism [6], [7], [23].

III. Wi-Fi HaLow Node Energy Consumption

A. Evaluation Experiments Setup

The test bench used to carry out the experiments is shown in Fig. 2. It consists of an AP, an STA and a server. The STA is associated to the AP and works as a CoAP client. It is regularly woken up to exchange frames with the server, which provides a CoAP service based on a ThingsBoard solution [37].

The STA is an evaluation kit (EVK) distributed by Silex Technology [38], and the AP is composed of a Raspberry Pi 3B+ and an Alfa Network APHI-7292 shield [39]. These solutions are built around a Newracom NRC-7292 chip and an RFFM-6901 front end module (FEM). The NRC-7292

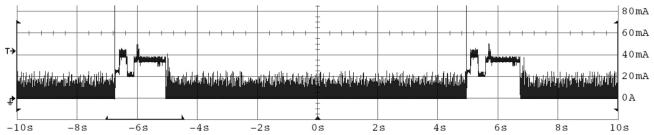

Fig. 3. Wake-up phases of a non-TIM STA.

contains an 802.11ah Wi-Fi System-on-Chip (SoC), two Cortex M0 and M3 processors, 32 kBytes of cache, flash memory, and all the interfaces needed to develop an IoT object [40]. The RFFM-6901 can amplify the signal up to 23 dBm [41].

Newracom provides a complete solution to develop test programs but all the mechanisms proposed by the task group (TGah) are not implemented. DCF and EDCA are integrated, while RAW and TWT are not. TIM, AID and NDP mechanisms are partially deployed, but not the PV1 headers, for security reasons [42].

In the experiments, the current drawn by the various STA components is measured by a Keysight CX3300 current analyzer. The AP broadcasts its SSID on channel 913.5 MHz, with a long GI, a bandwidth of 1 MHz and a beacon frame transmitted every 2s. The data exchanged is encoded in JSON and encapsulated in a CoAP/UDP/IPv4 packet.

Experiments are carried out for TIM and non-TIM mode, as described in Section II-D. The EVK's components are switched off during the sleep period, with the exception of the retention memory and the 32-MHz clock oscillator. The experimental station is configured to minimize power consumption and it works in standalone mode. In addition, a Raspberry Pi with an APHI-7292 shield spies the Wi-Fi HaLow exchanges. The frames are captured and visualized with WireShark to verify the state of the communication.

Experiments are made in a lab where environmental factors, such as temperature, are constant. The technical documentation indicates that the circuits can operate between −40 °C and 85 °C, at humidity levels ranging from 15 to 95%.

B. Non-TIM Station Power Consumption

In this experiment, the current drawn by the NRC-7292 chip and the RFFM-6901 amplifier is measured for a non-TIM mode. Transmit power is set to 0 dBm, MCS to 7 in automatic mode, and wake-up phases are set every 10s. The power measurements are performed on the STA with 165 bytes of CoAP data sent to the server (44 bytes of CoAP header and 121 bytes of JSON data), followed by the reception of a CoAP acknowledgment. Fig. 3 shows the current consumed by the STA for two consecutive wake-up phases.

The STA is woken up every 10s for an average duration of 1.7s. The evolution of the current drawn by the NRC-7292 chip and the amplifier during a wake-up is shown on Fig. 4 and detailed in Tables III and IV. In deep sleep state, the current consumed is measured at 18.13 μA.

At each wake-up, the device performs the following operations, noted (1) to (8) on Fig. 4: system and I/O initialization, FOTA check, PHY, RF, and MAC initialization, and FreeRTOS startup and internal task initialization. Connection information is stored in retention memory, allowing time-consuming MAC procedures, such as channel scanning, authentication, and association, to be skipped when reconnecting. Data transmission can be seen in Fig. 4 phase (9), with the current drawn by the amplifier. The STA first sends a QoS data frame to inform the AP of its wake-up status, followed by an ARP frame exchange. The station then transmits the CoAP data frame, which is subsequently acknowledged by the server. The transmission phase ends with the sending of a QoS frame, sent by the STA to inform the AP that it is returning to deep sleep. All frames are acknowledged by an NDP-Ack. During phase (9), the current consumed by the FEM to transmit data is equal to 112.50 mA and the current consumed to receive is equal to 34.53 mA.

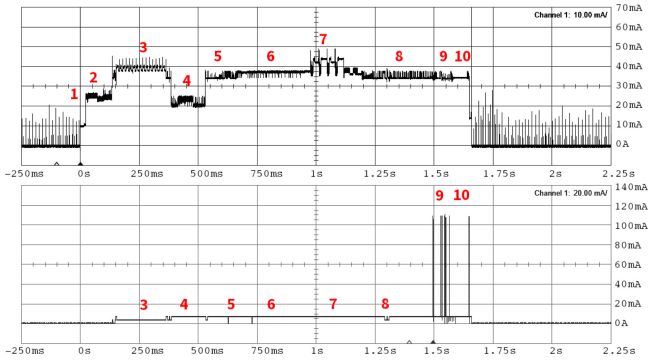

Fig. 4. NRC-7292 and FEM RFFM-6901 current measurement in a transmission phase of a non-TIM STA.

TABLE III
TIME AND CURRENT CONSUMED BY A NON-TIM STA DURING A WAKE UP

Phase	duration		current		
	variable	value	variable	NRC-7292 value	FEM value
(1)	t_{wu_1}	24 ms	I_{wu_1}	10.59 mA	0
(2)	t_{wu_2}	116 ms	I_{wu_2}	25.55 mA	0
(3)	t_{wu_3}	253 ms	I_{wu_3}	39.42 mA	3.16 mA
(4)	t_{wu_4}	148 ms	I_{wu_4}	20.02 mA	7.44 mA
(5)	t_{wu_5}	136 ms	I_{wu_5}	34.53 mA	7.44 mA
(6)	t_{wu_6}	326 ms	I_{wu_6}	38.24 mA	7.44 mA
(7)	t_{wu_7}	143 ms	I_{wu_7}	42.29 mA	7.44 mA
(8)	t_{wu_8}	385 ms	I_{wu_7}	34.53 mA	7.44 mA
(9)	t_{wu_9}	*	I_{wu_8}	34.53 mA	*
(10)	$t_{\mathrm{wu}_{10}}$	100 ms**	I_{wu_9}	34.53 mA	7.44 mA

* depends on the CoAP frames exchanged
** waiting time before deep sleep, defined in the program

TABLE IV
DURATION OF THE FRAMES TRANSMITTED BY A NON-TIM STA DURING A WAKE UP

Frame (x)	MPDU_x (bytes)	$N_{\mathrm{tx},x}$ / $N_{\mathrm{rx},x}$*	Frame duration	
			variable ($t_{x,mcs}$)	value
ARP	66	1/1	$t_{\mathrm{arp},10}$	4204 µs
NDP-ACK	0	2/4	$t_{\mathrm{ack},10}$	560 µs
CoAP (post)	231	1/0	$t_{\mathrm{coap},7}$**	1211 µs
CoAP (2.04)	70	0/1	$t_{\mathrm{coap},7}$	768 µs
QoS Data	30	2/0	$t_{\mathrm{qos},10}$	2293 µs

* number of frames transmitted and received during the phase (9)
** t_{coap} for the transmission of 165 bytes, MCS=7 and BW=1MHz

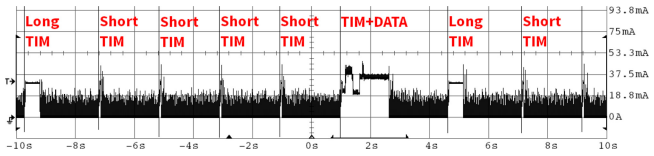

Fig. 5. Wake-up phases of a TIM STA.

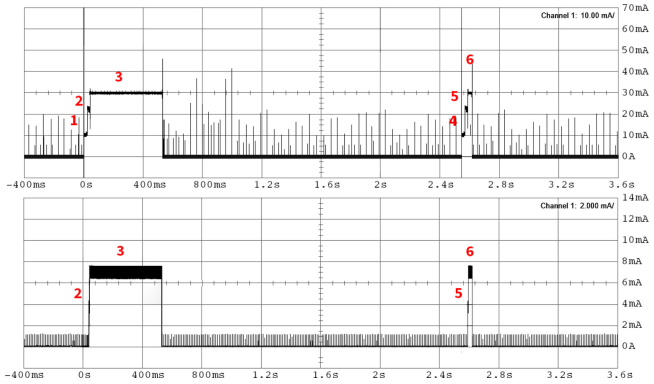

Fig. 6. Duration and current consumed by the STA when receiving TIM beacons.

TABLE V
TIME AND CURRENT CONSUMED BY AN STA TO RECEIVE TIM BEACONS

TIM Beacon	Phase	NRC-7292		FEM	
		duration	current	duration	current
Long	(1)	22 ms	9.38 mA	0	0
	(2)	20 ms	22.83 mA	4 µs	3.85 mA
	(3)	483 ms	29.78 mA	483 ms	7.03 mA
Short	(4)	22 ms	9.57 mA	0	0
	(5)	20 ms	22.72 mA	4 µs	3.72 mA
	(6)	30 ms	29.76 mA	30 ms	7.07 mA

C. TIM Station Power Consumption

In this experiment, the current drawn by the NRC-7292 chip and the RFFM-6901 amplifier is measured for a TIM mode. The TIM beacons are transmitted every 2s by the AP, the MCS is set to 7 in automatic mode and the transmit power to 0 dBm. The power measurements are performed on the STA with 138 bytes of CoAP data received from the server (17 bytes of CoAP header and 121 bytes of JSON data), followed by the transmission of a CoAP acknowledgment. Fig. 5 shows the current consumed by the STA for the different wake-ups.

The STA is woken up to receive each TIM beacon frame. The first one is a long TIM beacon, followed by five short TIM beacons transmitted every 2s. On the fifth one, the STA starts a full wake-up to receive 121 bytes of CoAP data. It is informed in the TIM beacon of the availability of the CoAP data frame. Fig. 6 shows the current drawn by the NRC-7292 chip and the RFFM-6901 amplifier when receiving a short and a long TIM beacon frame with the same time base. These measurements are detailed in Table V.

To receive TIM beacons, the STA is put into a μ code state, in which it consumes few resources and does not require to start the OS and load the UDP/IP stack. A short TIM frame takes 72 ms for 68 bytes and a long TIM frame takes 525 ms for 138 bytes. If the TIM beacons indicate a packet addressed to it, the STA initiates the transition to active mode.

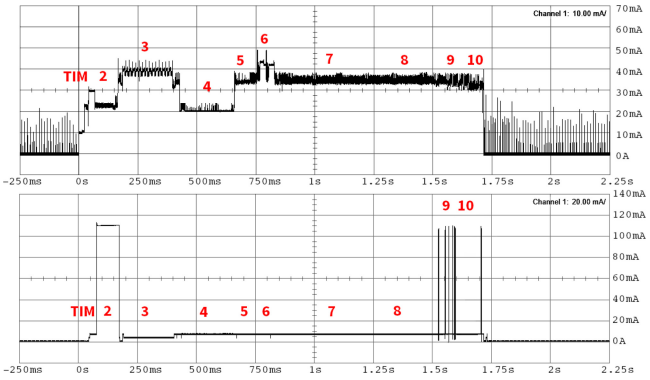

Fig. 7. NRC-7292 and FEM RFFM-6901 current measurement in a transmission phase of a TIM STA.

TABLE VI
TIME AND CURRENT CONSUMED BY A TIM STA DURING A WAKE UP

Phase	duration		current		
	variable	value	variable	NRC-7292 value	FEM value
TIM	(see table V)				
(2)	t_{wu_2}	98 ms	I_{wu_2}	23.67 mA	112,3 mA
(3)	t_{wu_3}	263 ms	I_{wu_3}	39,42 mA	3,16 mA
(4)	t_{wu_4}	232 ms	I_{wu_4}	20,00 mA	7,44 mA
(5)	t_{wu_5}	97 ms	I_{wu_5}	34,53 mA	7,44 mA
(6)	t_{wu_6}	71 ms	I_{wu_6}	42,29 mA	7,44 mA
(7-8)	t_{wu_7}	714 ms	I_{wu_7}	35,53 mA	7,44 mA
(9)	t_{wu_9}	*	I_{wu_9}	34,53 mA	*
(10)	t_{wu_10}	100ms**	I_{wu_10}	34,53 mA	7,44 mA

* depends on the CoAP frames exchanged
** waiting time before deep sleep, defined in the program

TABLE VII
DURATION OF THE FRAMES TRANSMITTED BY A TIM STA DURING A WAKE UP

Frame (x)	MPDU_x (bytes)	$N_{\mathrm{tx},x}$ / $N_{\mathrm{rx},x}$*	Frame duration	
			variable ($t_{x,mcs}$)	value
ARP	66	1/1	$t_{\mathrm{arp},10}$	4216 µs
NDP-ACK	0	2/4	$t_{\mathrm{ack},10}$	560 µs
CoAP (observable)	206	0/1	$t_{\mathrm{coap},7}$**	1129 µs
CoAP (ack)	70	1/0	$t_{\mathrm{coap},7}$	763 µs
QoS Data	30	2/0	$t_{\mathrm{qos},10}$	2287 µs

* number of frames transmitted and received during the phase (9)
** t_{coap} for the transmission of 138 bytes, MCS=7 and BW=1MHz

If not, the STA returns to deep sleep. Fig. 7 shows the current consumed by the NRC-7292 and the FEM when receiving a TIM beacon followed by a full wake-up and a data transfer with the same time base. Tables VI and VII contain the details of these measurements.

The transition from the μ code to the active mode includes the initialization of the different modules, the startup of the OS, the activation of the connection and the data transmission. If we compare Tables IV and VII, the duration and the current consumed by the NRC-7292 and the FEM during phases (3) to (10) are equal for TIM and non-TIM. During phase (2), the current consumed by the FEM is higher in TIM operation. This phase corresponds to the initialization of the STA and occurs just after the reception of the TIM beacon frame.

TABLE VIII
CURRENT CONSUMED BY THE FEM IN TRANSMISSION (FOR 3.3-V SUPPLY)

Tx Power (dBm)	FEM current I_{tx} (mA)
0	112.48
3	115.26
7	120.75
10	129.85
14	165.40
17	207.90
20	278.83
23	357.31

D. FEM Current Consumption

Previous measurements are made at 0 dBm and the current consumed by the FEM depends on the transmit power. In this experiment, the current consumed by the FEM is measured for several transmit power and the results are presented in Table VIII. The NRC-7292 chip's technical documentation indicates that the current drawn by the RFFM-6901 circuit is equal to 350 mA for a 23 dBm transmit power, which corresponds to our measurements with an error of less than 2% [40].

For a 0 dBm power, current consumption is equal to 112.50 mA. Up to 12 dBm, it remains below 150 mA, then increases exponentially to 350 mA for 23 dBm. The maximum distance between the STA and the AP depends on the transmission power. In the U.S., 23 dBm is authorized, which allows a distance of 1 km in MCS 10. In Europe, this power is limited to 14 dBm, which covers a distance of 500 m [33]. The energy consumed by a station during transmission depends on the transmit power and frame duration. The latter is directly linked to the MCS used, which in turn depends on distance and transmit power.

IV. ANALYSIS AND DISCUSSIONS ON THE ENERGY CONSUMPTION

A. Theoretical Analysis of the Energy Consumption

In this section, the measurement results are used to evaluate the lifetime of an STA according to its operating mode. The energy consumed during a wake-up is given by

$$E = E_{wu} + E_{tx} + E_{rx} \tag{1}$$

and the energy consumed per useful bit is given by

$$E_{bits} = \frac{E}{8 \cdot N_{DATA}} \tag{2}$$

where E, E_{bits}, E_{wu}, E_{tx}, and E_{rx} are the energy consumed by the STA in a complete wake-up phase, the energy consumed per useful bit, the energy consumed by the STA for the wake-up and initialization, for the transmission and for the reception, respectively. N_{DATA} is the number of data bytes transmitted by the STA during this round. Note that E_{wu} depends on the hardware. For the one used in this experiment, it can be calculated by

$$E_{wu} = V_{sta} \cdot \left(\sum_{i=1}^{8} I_{wu_i} \cdot t_{wu_i} + I_{wu_{10}} \cdot t_{wu_{10}} \right) \tag{3}$$

where V_{sta}, I_{wu_i}, and t_{wu_i} are the supply voltage, the sum of the current consumed by the NRC-7292 and the FEM, and the duration of each phase noted (1) to (8) and (10) in Tables III and VI, respectively. The energy consumed by the STA during the transmission and the reception are given by

$$\begin{aligned} E_{rx} &= V_{sta} \cdot I_{rx} \cdot t_{rx} \\ E_{tx} &= V_{sta} \cdot I_{tx} \cdot t_{tx} \end{aligned} \tag{4}$$

where I_{rx}, I_{tx}, t_{rx}, and t_{tx} are the current consumption and the duration of the transmission and reception phases. In this experiment, the STA is configured to wake up every 10s and exchange 121 bytes of CoAP data with the server. The duration of the transmission phase is given by

$$\begin{aligned} t_{tx} = {} & N_{tx,arp} \cdot t_{arp,10} + N_{tx,coap} \cdot t_{coap,mcs} \\ & + N_{tx,qos} \cdot t_{qos,10} + N_{tx,ack} \cdot t_{ack,10} \end{aligned} \tag{5}$$

where $N_{tx,arp}$, $N_{tx,ack}$, $N_{tx,coap}$, $N_{tx,qos}$, $t_{ack,10}$, $t_{arp,10}$, $t_{coap,mcs}$, and $t_{qos,10}$ are the number of frames transmitted by the STA and the duration of each frame, respectively. The values are detailed in Tables IV and VII. The reception duration depends on the duration of the frames received and the waiting times of the CSMA/CA mechanism. The reception duration is given by

$$\begin{aligned} t_{rx} = {} & N_{rx,arp} \cdot \left(t_{difs} + t_{rx,arp} + t_{sifs}\right) \\ & + N_{tx,arp} \cdot \left(t_{difs} + t_{sifs} + t_{ack,10}\right) \\ & + N_{rx,coap} \cdot \left(t_{difs} + t_{coap,mcs} + t_{sifs}\right) \\ & + N_{tx,coap} \cdot \left(t_{difs} + t_{sifs} + t_{ack,10}\right) \\ & + N_{tx,qos} \cdot \left(t_{difs} + t_{sifs} + t_{ack,10}\right) \end{aligned} \tag{6}$$

where t_{difs} and t_{sifs} are the distributed interframe space (DIFS) and the short interframe space (SIFS) [36]. The frames duration ($t_{arp,10}$, $t_{coap,mcs}$ and $t_{qos,10}$) are given by

$$t_{x,mcs} = t_{phy} + t_{sym} \cdot \left\lceil \frac{8 \cdot \text{MPDU}_x + N_{serv} + N_{tail} \cdot N_{es}}{N_{dbps}} \right\rceil \tag{7}$$

where $t_{x,mcs}$, t_{sym}, and t_{phy} are the duration of the frame x, the duration of an OFDM symbol, and the duration of the PHY header, respectively. MPDU_x, N_{dbps}, N_{serv}, N_{tail} and N_{es} are the MAC Protocol Data Unit, the number of data bits per symbol, the number of bits in the service field, the number of BCC encoders and the number of tail bits per BCC encoder. The OFDM symbol is equal to 40 μs for a long guard interval and 36 μs for a short guard. The PHY header is 560 μs for 1-MHz BW and 240 μs for 2-MHz BW. Tables IV and VII contain the values of MPDU_x, x is the frame type. ARP, NDP-Ack, and QoS-data frames are transmitted with the minimum MCS, which is 10 for 1-MHz BW and 0 for 2-MHz BW. The CoAP frames are transmitted with the best MCS according to the distance and N_{dbps} depends on both the bandwidth and the MCS used [5], [36]. $N_{dbps} = 6$ for MCS10 and 1-MHz BW, 120 for MCS7. $N_{dbps} = 26$ for MCS0 and 2-MHz BW, 260 for MCS7 [5], [36]. $N_{serv} = 8$ bits, $N_{es} = 1$ and $N_{tail} = 6$ bits [5], [36].

Table IX contains the duration values of frames exchanged between the CoAP client and server. Theoretical values

TABLE IX
THEORETICAL AND MEASURED VALUES FOR THE DURATION OF FRAMES EXCHANGED BETWEEN COAP CLIENT AND SERVER

Frames (x)	Frame duration		
	theoretical value	non-TIM practical value	TIM practical value
ARP	4200 µs	4204 µs	4216 µs
NDP-ACK	560 µs	560 µs	560 µs
CoAP (post)	1200 µs	1211 µs	-
CoAP (observable)	1120 µs	-	1129 µs
CoAP (ack)	760 µs	768 µs	763 µs
QoS Data	2280 µs	2293 µs	2287 µs

are obtained with (7), and measured values come from Tables IV and VII.

Theoretical values validate experimental measurements. The energy consumed by a station is directly related to the duration of the frames exchanged between the various devices, and this duration depends on the amount of data to be transmitted and the MCS used.

B. Station Lifetime Prediction

To determine station lifetime, it is necessary to calculate the time and energy consumed in one operating cycle, as follows:

$$t_{\text{cyc}} = t_{\text{wu}} + t_{\text{tx}} + t_{\text{rx}} + t_{\text{sleep}} \tag{8}$$

$$\begin{aligned} E_{\text{cyc,tim}} = {} & E_{\text{wu}} + E_{\text{tx}} + E_{\text{rx}} \\ & + \frac{t_{\text{sleep}}}{t_{\text{tbtt}}}\left(\frac{1}{N_{\text{tim}}}\left(E_{\text{dtim}} + (t_{\text{tbtt}} - t_{\text{dtim}}) \cdot V_{\text{sta}} \cdot I_{\text{sleep}}\right)\right) \\ & + \frac{t_{\text{sleep}}}{t_{\text{tbtt}}}\left(\frac{N_{\text{tim}} - 1}{N_{\text{tim}}}\left(E_{\text{tim}} + (t_{\text{tbtt}} - t_{\text{tim}}) \cdot V_{\text{sta}} \cdot I_{\text{sleep}}\right)\right) \end{aligned} \tag{9}$$

$$E_{\text{cyc,ntim}} = E_{\text{wu}} + E_{\text{tx}} + E_{\text{rx}} + V_{\text{sta}} \cdot I_{\text{sleep}} \cdot t_{\text{sleep}} \tag{10}$$

where t_{cyc}, $E_{\text{cyc,tim}}$, and $E_{\text{cyc,ntim}}$ are the duration and the energy consumed by an STA during a cycle in TIM or non-TIM modes, respectively. t_{wu}, t_{sleep} and t_{tbtt} correspond to the duration of the wake up phases, noted (1) to (8) on Figs. 4 and 7, the duration of the deep sleep state and the time between two beacon frames. N_{tim} is the number of beacon frames separating two DTIMs. E_{dtim} and E_{tim} are the energy consumed by an STA to receive TIM and DTIM beacons and I_{sleep} is the current consumed by the STA during deep sleep.

The STA lifetime duration is then calculated by

$$t_{\text{life}} = \frac{E_{\text{src}} \cdot t_{\text{cyc}}}{E_{\text{cyc}}} \tag{11}$$

where t_{life} and E_{src} are the STA lifetime estimation and the energy provided by the power source, respectively.

To transmit or receive 121 data bytes every 10s, the low-power STA consumes 322 mJ in TIM mode and 226 mJ in non-TIM mode. These results are obtained with (1), (9), and (10), and the values in Tables III–VII. Table X shows the energy consumption and lifetime of a station powered by a standard 2000 mAh battery, for different duty cycles. The values are calculated for a TIM beacon transmitted every 2s and a DTIM beacon every 5 TIM beacons.

TABLE X
ENERGY CONSUMED BY AN STA IN TIM AND NON-TIM MODES

duty cycle	Mode	Energy consumed			Station Lifetime
		TIM (mJ)	wake-up (mJ)	deep-sleep (mJ)	(days)
10s	non-TIM	0	225.70	0.604	13.25
	TIM	72.46	248.96	0.555	9.31
60s	non-TIM	0	225.70	3.62	78.48
	TIM	434.77	248.96	3.33	26.19
15min	non-TIM	0	225.70	54.38	963.99
	TIM	6521.63	248.96	49.95	39.58

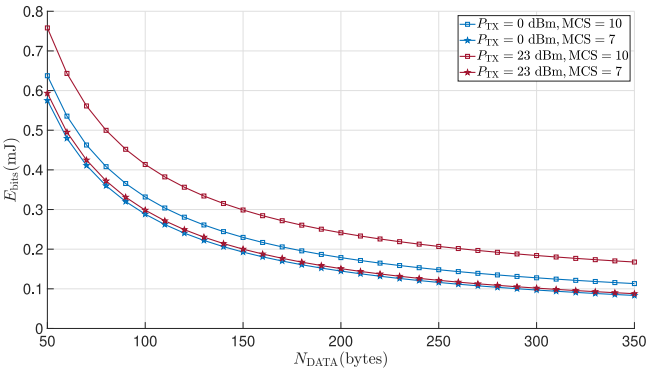

Fig. 8. Energy consumed by STA per useful bit versus number of data bytes transmitted (1-MHz BW).

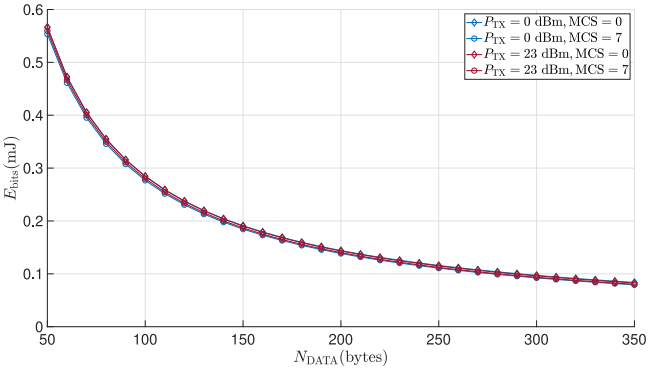

Fig. 9. Energy consumed by STA per useful bit versus number of data bytes transmitted (2-MHz BW).

Lifetime depends on the current drawn by the STA, the wake-up duration, the duty cycle and the number of wake-ups required to receive TIM and DTIM beacons. For the non-TIM mode, the battery life is equal to 78 days for a wake-up every 60s and more than 2 years for a wake-up every 15min. Lifetime increases in the same ratio as the duty cycle. For the TIM mode, the battery life is equal to 26 days for a wake-up every 60s and 39 days for a wake-up every 15min. Compared with a 10s operating cycle, lifetime increases by a ratio of 3 and 4, due to the reception of TIM and DTIM beacons every 2s. It should be note that this lifetime model does not take into account the behavior of the power source. In the case of battery power, performance can be strongly affected by the environment, in particular by temperature [43], [44]. Modeling the power source is outside the scope of this article.

C. Energy Consumption Per Useful Bit

Figs. 8 and 9 show the energy per useful bit consumed by the low-power STA as a function of the number of carried out data bytes, for 1 and 2-MHz BWs, respectively. These curves are based on (2) and consider only the energy consumed during a wake-up/transmission phase. The payload varies from 50 to 350 bytes, the transmission power is set to 0 and 23 dBm and the communication is in one direction only.

The energy consumed per useful bit decreases with the payload, in a ratio of one fifth to one seventh between a load of 50 and 350 bytes. When the load exceeds 150 bytes, the energy is less than 0.3 mJ. With a load of 350 bytes, that corresponds to the maximum payload if we consider the CoAP header, the energy consumed per useful bit is below 0.2 or even 0.1 mJ. The curves show that MCS, bandwidth and transmission power have little influence on energy consumption. This means that the energy consumed during start-up is not negligible compared with the energy consumed during transmission, with a ratio of one twentieth. The duration of an OFDM symbol is doubled for MCS10, which explains the difference observed in Fig. 8.

D. Discussions on the Energy Consumption

In this work, we qualify the energy consumed by an STA in a deep sleep mode for both TIM and non-TIM operation. In TIM, the STA consumes more energy for the same amount of data transmitted because it must wake up to receive the beacons. However, the TIM use case is different from the non-TIM one, as detailed in Section II-D1. The results of our measurements show that there are three ways to improve energy efficiency. The first one is to reduce the reboot time and the OS startup. The second one is to precisely define the wake-up cycle according to the use case and the time between each TIM beacon. The last one is to increase the amount of data transmitted per wake-up phase. Different solutions exist in the standard and need to be evaluated. A device can aggregate multiple frames into one, which reduces transmission time by adding a single header for all frames and fewer waking up phases. The maximum length of a single MPDU is 511 bytes, and the maximum length of an Aggregate MAC Protocol Data Unit (A-MPDU) is 511 symbols. Transmission opportunity (TxOP) is another solution. This QoS concept allows an STA to access the media for a longer and limited duration. This duration ranges between 1504 and 3008 μs depending on the traffic class [35]. Finally, TWT is a new media access method that minimizes energy consumption by negotiating contention-free slots between the AP and the STA. These mechanisms are intended to provide fair access time and are expected to increase energy efficiency. We plan to evaluate them in practice in future work.

The 802.11ah protocol has been defined to provide long range and low-power IoT solution to the Wi-Fi standard. Therefore, BW is divided by 10 in the sub-1 GHz frequency bands to increase coverage, so it can be classified as an LP-WAN without reaching the tens of kilometers covered by these technologies. The current that is consumed by a legacy Wi-Fi device is very similar to the current measured in this study for a 802.11ah protocol. Nevertheless, a 802.11ah device can transmit at a lower power to reach the same distances, which implies that it consumes less energy [45], [46], [47], [48], [49], [50], [51].

If we compare the Wi-Fi HaLow with an open LP-WAN protocol, such as LoRaWAN, we see that the energy consumed is similar to the 802.11ah at the same distance [52], [53]. For small packet, the LoRa protocol is better suited as it consumes less energy. For large volumes of data, 802.11ah is more efficient as it consumes less energy per transmitted useful bit [33], [52].

Wi-Fi HaLow is a very interesting IoT solution with high-data throughput and low latency. It can be easily integrated into existing Wi-Fi networks, natively supports the TCP/IP layer and embeds the latest security mechanisms.

V. Conclusion

In this article, we qualify the energy efficiency of the 802.11ah using the only hardware currently available on the market. This hardware is an EVK, which explains why not all the mechanisms recommended by the standard have been implemented. Nevertheless, our measurements demonstrate the feasibility of using IEEE 802.11ah as an ultralow-power IoT technology. The energy consumed per useful bit is less than 0.3 mJ for a payload greater than 150 bytes of data, and the battery lifetime can reach several years depending on the device's wake-up settings. Wi-Fi HaLow is the only IoT protocol that offers low power and high throughput while providing an end-to-end IP stack. For all of those reasons, it is a good candidate for IoT applications.

References

[1] E. Khorov, A. Lyakhov, A. Krotov, and A. Guschin, "A survey on IEEE 802.11ah: An enabling networking technology for smart cities," *Comput. Commun.*, vol. 58, pp. 53–69, May 2015. [Online]. Available: http://dx.doi.org/10.1016/j.comcom.2014.08.008

[2] L. Qiao, Z. Zheng, W. Cui, and L. Wang, "A survey on Wi-Fi HaLow technology for Internet of Things," in *Proc. 2nd IEEE Conf. Energy Internet Energy Syst. Integr.*, 2018, pp. 1–5.

[3] M. Park, "IEEE 802.11ah: Sub-1-GHz license-exempt operation for the Internet of Things," *IEEE Commun. Mag.*, vol. 53, no. 9, pp. 145–151, Sep. 2015.

[4] E. Khorov, A. Krotov, and A. Lyakhov, "Modelling machine type communication in IEEE 802.11ah networks," in *Proc. IEEE Int. Conf. Commun. Workshop (ICCW)*, 2015, pp. 1149–1154.

[5] V. Baños-Gonzalez, M. S. Afaqui, E. Lopez-Aguilera, and E. Garcia-Villegas, "IEEE 802.11ah: A technology to face the IoT challenge," *Sensors*, vol. 16, no. 11, p. 1960, 2016.

[6] L. Tian, S. Santi, A. Seferagić, J. Lan, and J. Famaey, "Wi-Fi HaLow for the Internet of Things: An up-to-date survey on IEEE 802.11ah research," *J. Netw. Comput. Appl.*, vol. 182, May 2021, Art. no. 103036.

[7] N. Ahmed, D. De, F. A. Barbhuiya, and M. I. Hussain, "MAC protocols for IEEE 802.11ah-based Internet of Things: A survey," *IEEE Internet Things J.*, vol. 9, no. 2, pp. 916–938, Jan. 2022.

[8] M. S. Meera and S. N. Rao, "A survey of the state of the art of 802.11ah," in *Proc. IEEE Int. Conf. Comput. Intell. Comput. Res. (ICCIC)*, 2018, pp. 1–4.

[9] R. M. V. Wessel and H. J. D. Vries, "Business impacts of international standards for information security management. lessons from case," *ICT Stand.*, vol. 1, pp. 25–40, Jan. 2013.

[10] T. Adame, A. Bel, B. Bellalta, J. Barcelo, and O. Miquel, "IEEE 802.11AH: The Wi-Fi approach for M2M communications," *IEEE Wireless Commun.*, vol. 21, no. 6, pp. 144–152, Dec. 2014.

[11] T. Adame, A. Bel, B. Bellalta, J. Barcelo, J. Gonzalez, and M. Oliver, "Capacity analysis of IEEE 802.11ah WLANs for M2M communications," in *Proc. 6th Int. Workshop Multiple Access Commun.*, 2013, pp. 139–155.

[12] Y. Zhao, O. N. C. Yilmaz, and A. Larmo, "Optimizing M2M energy efficiency in IEEE 802.11ah," in *Proc. IEEE Globecom Workshops (GC Wkshps)*, 2015, pp. 1–6.

[13] C. Kai, J. Zhang, X. Zhang, and W. Huang, "Energy-efficient sensor grouping for IEEE 802.11ah networks with max-min fairness guarantees," *IEEE Access*, vol. 7, pp. 102284–102294, 2019.

[14] T. Kim, D. Qiao, and W. Choi, "Energy-efficient scheduling of Internet of Things devices for environment monitoring applications," in *Proc. IEEE Int. Conf. Commun.*, 2018, pp. 1–7.

[15] U. Sangeetha and A. V. Babu, "Fair and efficient resource allocation in IEEE 802.11ah WLAN with heterogeneous data rates," *Comput. Commun.*, vol. 151, pp. 154–164, Feb. 2020. [Online]. Available: https://doi.org/10.1016/j.comcom.2019.12.043

[16] Q. T. Ngo, D. N. Dang, and Q. Le-Trung, "Extreme power saving directional MAC protocol in IEEE 802.11ah networks," *IET Netw.*, vol. 9, no. 4, pp. 180–188, 2020.

[17] Y. Wang, Y. Li, K. K. Chai, Y. Chen, and J. Schormans, "Energy-aware adaptive restricted access window for IEEE 802. 11ah based networks," in *Proc. IEEE 26th Annu. Int. Symp. Pers., Indoor Mobile Radio Commun.*, 2016, pp. 1211–1215.

[18] W. Yanru, Y. Li, K. K. Chai, Y. Chen, and J. Schormans, "Energy-aware adaptive restricted access window for IEEE 802.11ah based smart grid networks," in *Proc. IEEE Int. Conf. Smart Grid Commun., SmartGridComm*, 2016, pp. 581–586.

[19] Y. Wang, K. K. Chai, Y. Chen, J. Schormans, and J. Loo, "Energy-aware restricted access window control with retransmission scheme for IEEE 802.11ah (Wi-Fi HaLow) based networks," in *Proc. 13th Annu. Conf. Wireless Demand Netw. Syst. Services (WONS)*, 2017, pp. 69–76.

[20] V. Agarwal, R. A. Decarlo, and L. H. Tsoukalas, "Modeling energy consumption and lifetime of a wireless sensor node operating on a contention-based MAC protocol," *IEEE Sensors J.*, vol. 17, no. 16, pp. 5153–5168, Aug. 2017.

[21] L. Beltramelli, P. Osterberg, U. Jennehag, and M. Gidlund, "Hybrid MAC mechanism for energy efficient communication in IEEE 802.11ah," in *Proc. IEEE Int. Conf. Ind. Technol.*, 2017, pp. 1295–1300.

[22] N. Ahmed and M. I. Hussain, "Periodic traffic scheduling for IEEE 802.11ah networks," *IEEE Commun. Lett.*, vol. 24, no. 7, pp. 1510–1513, Jul. 2020.

[23] D. Bankov, E. Khorov, A. Lyakhov, and E. Stepanova, "Clock drift impact on target wake time in IEEE 802.11ax/ah networks," in *Proc. 5th Int. Conf. Eng. Telecommun. (EnT-MIPT)*, 2018, pp. 30–34.

[24] T.-L. Kao, H.-C. Wang, C.-H. Lu, and T.-H. Cheng, "An energy consumption evaluation of non-TIM strategy in IEEE 802.11ah," *IOP Conf. Ser. Mater. Sci. Eng.*, vol. 644, May 2019, Art. no. 012008.

[25] M. Shafiq et al., "Multiple access control for cognitive radio-based IEEE 802.11ah networks," *Sensors*, vol. 18, no. 7, pp. 1–28, 2018.

[26] L. Zheng, L. Cai, J. Pan, and M. Ni, "Performance analysis of grouping strategy for dense IEEE 802.11 networks," in *Proc. IEEE Glob. Telecommun. Conf. (GLOBECOM)*, 2013, pp. 219–224.

[27] A. Bel, T. Adame, B. Bellalta, J. Barcelo, J. Gonzalez, and M. Oliver, "CAS-based channel access protocol for IEEE 802.11ah WLANs," in *Proc. 20th Eur. Wireless Conf. (EW)*, 2014, pp. 1–6.

[28] D. Bankov, E. Khorov, A. Lyakhov, and J. Famaey, "Resource allocation for machine-type communication of energy-harvesting devices in Wi-Fi HaLow networks," *Sensors*, vol. 20, no. 9, p. 2449, 2020.

[29] X. Zhang and K. L. Yeung, "LLE: A timer extension mechanism for alarm-triggered traffic in IEEE 802.11ah WLANs," in *Proc. IEEE Int. Conf. Commun.*, 2017, pp. 1–6.

[30] A. J. Gopinath and B. Nithya, "Mathematical and simulation analysis of contention resolution mechanism for IEEE 802.11ah networks," *Comput. Commun.*, vol. 124, pp. 87–100, Jun. 2018. [Online]. Available: https://doi.org/10.1016/j.comcom.2018.04.006

[31] A. Kureev, D. Bankov, E. Khorov, and A. Lyakhov, "Improving efficiency of heterogeneous Wi-Fi networks with joint usage of TIM segmentation and restricted access window," in *Proc. IEEE 28th Int. Symp. Pers., Indoor Mobile Radio Commun. (PIMRC)*, 2018, pp. 1–5.

[32] I.-G. Lee et al., "WiFi HaLow for long-range and low-power Internet of Things: System on chip development and performance evaluation," *IEEE Commun. Mag.*, vol. 59, no. 7, pp. 101–107, Jul. 2021.

[33] S. Maudet, G. Andrieux, R. Chevillon, and J.-F. Diouris, "Practical evaluation of Wi-Fi HaLow performance," *Internet Things*, vol. 24, Dec. 2023, Art. no. 100957. [Online]. Available: https://www.sciencedirect.com/science/article/pii/S2542660523002809

[34] O. Raeesi, J. Pirskanen, A. Hazmi, J. Talvitie, and M. Valkama, "Performance enhancement and evaluation of IEEE 802.11ah multi-access point network using restricted access window mechanism," in *Proc. IEEE Int. Conf. Distrib. Comput. Sens. Syst. (DCOSS)*, 2014, pp. 287–293.

[35] Y. Cheng, D. Yang, H. Zhou, and H. Wang, "Adopting IEEE 802.11 MAC for industrial delay-sensitive wireless control and monitoring applications: A survey," *Comput. Netw.*, vol. 157, pp. 41–67, Jul. 2019. [Online]. Available: https://doi.org/10.1016/j.comnet.2019.04.002

[36] *IEEE Standard for Information Technology–Telecommunications and Information Exchange Between Systems—Local and Metropolitan Area Networks–Specific Requirements—Part 11: Wireless LAN Medium Access Control (MAC) and Physical Layer (PHY) Specifications Amendment 2: Sub 1 GHz License Exempt Operation*, IEEE Standard 802.11ah-2016 (Amendment to IEEE Standard 802.11-2016, as amended by IEEE Standard 802.11ai-2016), 2017.

[37] "Thingsboard." Accessed: Jan. 30, 2024. [Online]. Available: https://thingsboard.io/

[38] (Silex Technol. Inc. Co., Seika, Japan). *SX-NEWAH Evaluation Kit*. Accessed: Jan. 30, 2024. [Online]. Available: https://www.silextechnology.com/connectivity-solutions/embedded-wireless/sx-newah-evaluation

[39] "Ahpi-7292s: Network." Accessed: Jan. 30, 2024. [Online]. Available: https://www.alfa.com.tw/products/ahpi7292s

[40] "Newracom nrc-7292." Accessed: Jan. 30, 2024. [Online]. Available: https://newracom.com/products/nrc7292

[41] "2.8 to 4.2 V, 915-MHz ISM band transmit/receive module with diversity switch," Data Sheet RFFM6901, Qorvo Wireless Co., Greensboro, NC, USA, 2015. [Online]. Available: https://www.qorvo.com/products/p/RFFM6901

[42] "Newracom github." Accessed: Jan. 30, 2024. [Online]. Available: https://github.com/newracom

[43] K. Hasan, N. Tom, and M. R. Yuce, "Navigating battery choices in IoT: An extensive survey of technologies and their applications," *Batteries*, vol. 9, no. 12, p. 580, 2023. [Online]. Available: https://www.mdpi.com/2313-0105/9/12/580

[44] W. Zhou, Y. Zheng, Z. Pan, and Q. Lu, "Review on the battery model and SOC estimation method," *Processes*, vol. 9, no. 9, p. 1685, 2021. [Online]. Available: https://www.mdpi.com/2227-9717/9/9/1685

[45] A. Garcia-Saavedra, P. Serrano, A. Banchs, and G. Bianchi, "Energy consumption anatomy of 802.11 devices and its implication on modeling and design," in *Proc. 8th Int. Conf. Emerg. Netw. Exp. Technol.*, 2012, pp. 169–180. [Online]. Available: https://doi.org/10.1145/2413176.2413197

[46] S.-L. Tsao and C.-H. Huang, "A survey of energy efficient MAC protocols for IEEE 802.11 WLAN," *Comput. Commun.*, vol. 34, no. 1, pp. 54–67, 2011. [Online]. Available: https://www.sciencedirect.com/science/article/pii/S014036641000424X

[47] D. Halperin, B. Greenstein, A. Sheth, and D. Wetherall, "Demystifying 802.11n power consumption," in *Proc. Int. Conf. Power Aware Comput. Syst.*, 2010, pp. 1–5.

[48] S. Keranidis, G. Kazdaridis, N. Makris, T. Korakis, I. Koutsopoulos, and L. Tassiulas, "Experimental evaluation and comparative study on energy efficiency of the evolving IEEE 802.11 standards," in *Proc. 5th Int. Conf. Future Energy Syst.*, 2014, pp. 109–119. [Online]. Available: https://doi.org/10.1145/2602044.2602069

[49] C.-Y. Li et al., "An energy efficiency perspective on rate adaptation for 802.11n NIC," *IEEE Trans. Mobile Comput.*, vol. 15, no. 6, pp. 1333–1347, Jun. 2016.

[50] P. Silva, N. T. Almeida, and R. Campos, "A comprehensive study on enterprise Wi-Fi access points power consumption," *IEEE Access*, vol. 7, pp. 96841–96867, 2019.

[51] Y. Zeng, P. H. Pathak, and P. Mohapatra, "A first look at 802.11ac in action: Energy efficiency and interference characterization," in *Proc. IFIP Netw. Conf.*, 2014, pp. 1–9.

[52] L. Casals, B. Mir, R. Vidal, and C. Gomez, "Modeling the energy performance of LoRaWAN," *Sensors*, vol. 17, no. 10, p. 2364, 2017. [Online]. Available: https://www.mdpi.com/1424-8220/17/10/2364

[53] S. Maudet, G. Andrieux, R. Chevillon, and J.-F. Diouris, "Refined node energy consumption modeling in a LoRaWAN network," *Sensors*, vol. 21, no. 19, p. 6398, 2021. [Online]. Available: https://www.mdpi.com/1424-8220/21/19/6398